Int. J. Electron. Commun. (AEÜ) 142 (2021) 153981

Contents lists available at ScienceDirect

International Journal of Electronics and Communications

journal homepage: www.elsevier.com/locate/aeue

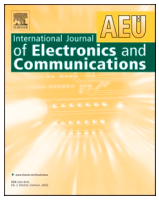

Regular paper

Low-profile UWB antenna with unidirectional radiation pattern analyzed with the theory of characteristic modes

Carlos Ramiro Peñafiel-Ojeda [a,b], Marta Cabedo-Fabrés [b], Aníbal Llanga-Vargas [b], Miguel Ferrando-Bataller [b,*]

[a] G-RESEARCH, Universidad Nacional de Chimborazo (UNACH), 060110 Riobamba, Ecuador
[b] Instituto de Telecomunicaciones y Aplicaciones Multimedia (ITEAM), Universitat Politècnica de València, 46022 Valencia, Spain

ARTICLE INFO

Keywords:
Low profile
Polarization diversity
Theory of characteristics modes
Unidirectional radiation pattern
UWB

ABSTRACT

This paper presents a low-profile Ultra Wide Band (UWB) antenna with polarization diversity for new 5G base stations. The antenna consists of a metallic ring capacitively fed with four circular monopoles and reinforced with a cylindrical cavity to generate a unidirectional radiation pattern. The Theory of Characteristic Modes is used to analyze and explain the behaviour of the proposed antenna excited with differential feeding configurations. A prototype of the optimized design has been manufactured and measured, yielding good impedance matching (S_{11}<-10 dB) from 3 GHz to 6 GHz with maximum directivity of 10.51 dBi. Measured and simulated results are in good agreement.

1. Introduction

In current mobile communication systems, the data traffic of the indoor communication far exceeds that of the outdoor link. There is a growing interest in base stations that can be installed inside buildings, in order to increase capacity and transmission speed. Outdoor base stations are vertical arrays of dual polarized elements, which have sectorial radiation patterns, usually 120°, and are installed on communications towers. In indoor environments, low-profile, dual-polarized antennas are required to be installed normally on the ceiling of the rooms. A good state of the art of antennas for 5G systems has been carried out at [1], the antenna presented here can be classified as Ultra-wide Band MIMO.

This paper is oriented towards improving the performance of indoor base stations, especially the bandwidth and the stability of the radiation patterns, but the fundamental innovation is the use of the Characteristic Modes theory to systematize design. The proposed design will be compared with the recent publications listed below. All designs are unidirectional and have in common that they are center-fed cavities with crossed dipoles or structures capable of achieving circular polarization.

As a starting point, the most recent publications with specifications similar to those proposed have been studied. We start by reviewing several references of antennas with unidirectional radiation, high bandwidth and dual polarization. The radiating elements of the paper [2] are crossed dipoles in front of a cavity, achieve a bandwidth of 1710–2690 MHz. The design of paper [3] using shorted dipoles has a bandwidth from 1.69 to 3.7 GHz. The reference [4] uses dual-polarized magneto-electric dipole elements, a wide impedance bandwidth from 1.6 to 3.7 GHz is obtained, but the 3D radiating elements are difficult to implement.

Low profile and circularly polarized references are reviewed below, which are also intended for indoor coverage, have only one input port, so they lose the MIMO capability, but they achieve good bandwidths. The paper "Wideband Circularly Polarized Cross-Dipole Antenna" [5] achieves bandwidth of 1.99–3.22 GHz. The reference [6] features a circularly polarized design with crossed dipoles and a coupling element, the achieved bandwith is 2.05 to 3.72 GHz. Finally, a good bandwidth and circular polarization are also achieved in the paper [7],however, the manufacturing is complex and it does not have MIMO capability, since it has only one polarization.

This paper presents a UWB antenna consisting of 4 circular monopoles placed in front of a cylindrical cavity. The final design achieves high bandwidth, with differential feeding and and the radiated fields have dual polarization.The design is based on the Characteristic Modes Theory and the authors' experience in UWB planar antenna design [8]. The most important innovations of the paper are related to the study of open cylindrical cavity modes, including the effect of feeding structures, which are also analyzed with modal analysis, the authors presented

* Corresponding author at: Universitat Politècnica de València, Camino de Vera s/n, Valencia, Spain.
E-mail addresses: carlospenafiel@unach.edu.ec (C.R. Peñafiel-Ojeda), mferrand@dcom.upv.es (M. Ferrando-Bataller).

https://doi.org/10.1016/j.aeue.2021.153981
Received 30 June 2021; Accepted 20 September 2021
Available online 8 October 2021

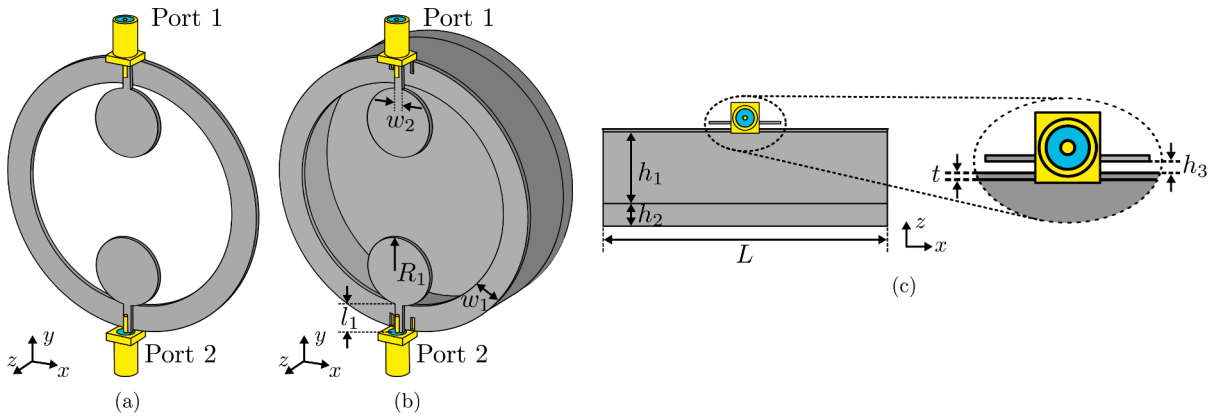

Fig. 1. (a) Model A: Metallic ring with differential feeding, (b) Model B: Cavity backed metallic ring with differential feeding, (c) Lateral view of Model B. Optimized parameters: $L = 64$ mm, $l_1 = 6.5$ mm, $w_1 = 6$ mm, $w_2 = 1.9$ mm, $R_1 = 8$ mm, $h_1 = 15$ mm, $h_2 = 5$ mm, $h_3 = 0.6$ mm, $t = 0.035$ mm.

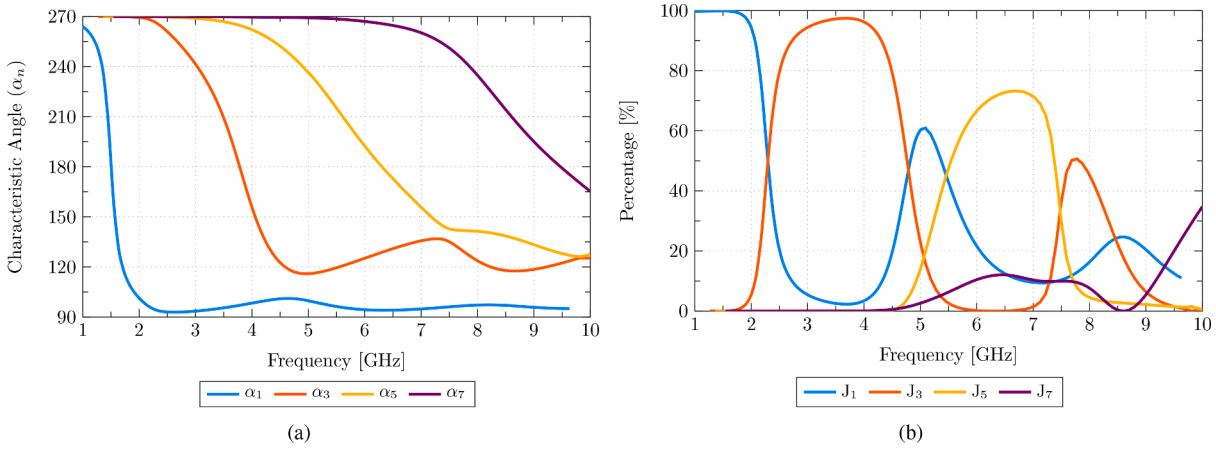

Fig. 2. Characteristic current distribution and radiation patters of the even characteristic modes of Model A at resonance frequency: (a) J_1 at 1.5 GHz, (b) J_3 at 3.78 GHz, (c) J_5 at 6.3 GHz and (d) J_7 at 9.47 GHz.

preliminary results in in [9].

The Theory of Characteristic Modes (TCM), first proposed by R.F. Harrington and Garbacz [10], was revised by some of the authors of this paper in 2007 [8]. This theory has gained a lot of interest for the design of broadband antennas in the last decade, because of the physical interpretation it brings about the radiation of the antenna.

In this work, the TCM is used to get information about the resonance frequency, current distribution, radiation pattern and power contribution of the modes that are excited on the proposed antenna. Due to the complexity of the structure, a modal analysis of a simplified version of the antenna without the cavity is first presented. Next, the complete antenna is analyzed and optimized with the help of the TCM.

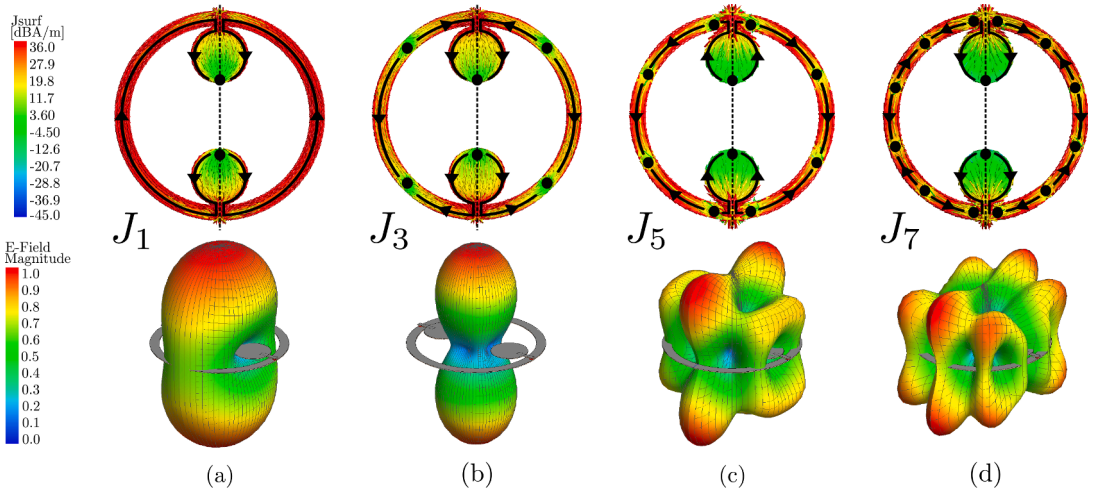

Fig. 3. (a) Characteristic angle variation for the first odd modes of Model A and modal radiation patterns at resonance frequency, (b) Contribution of the odd characteristic modes of Model A to the total radiated power when the antenna is fed with differential excitation.

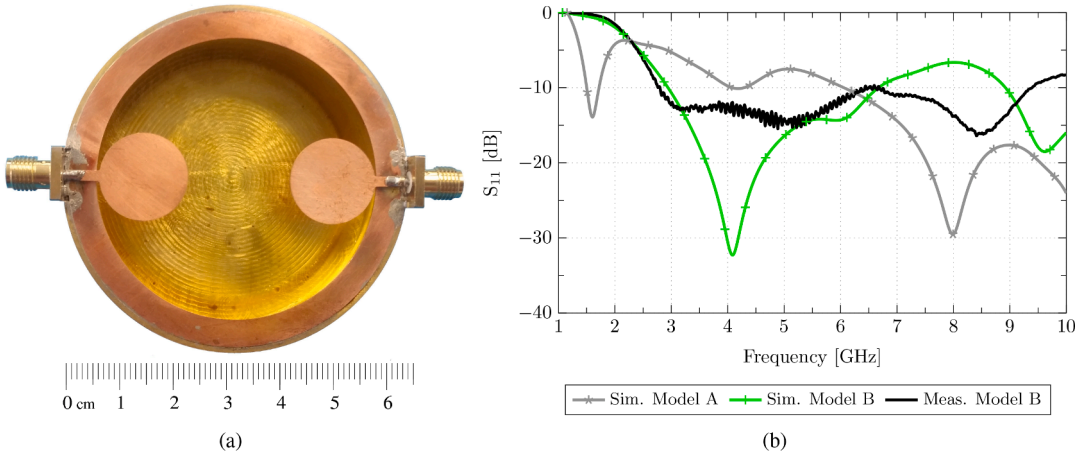

Fig. 4. (a) Top view of manufactures Model B proposed antenna, and (b) Simulated S_{11} parameter of Model A, and simulated and measured S_{11} parameter of Model B.

Furthermore, the work describes the manufacturing and measurement of a prototype of the antenna with polarization diversity, and includes a comparison between simulated and experimental results. The paper ends with the conclusions.

2. Modal Analysis of a Circular Ring Antenna

For the sake of clarity, let us begin analysing the simplified version of the antenna (Model A) presented in Fig. 1(a). This model includes only the circular ring, two circles are also added, which will consider the effect of the two input ports.

The modal solution of the fields and currents in flat circular loops are known [11]. The distribution of currents over the circular structure is a periodic function. The numbering of the modes depends on the number of periods of the function. The polarization of the radiated fields is also important. In the analyzed antennas, the radiated electric field will be considered to have vertical polarization (Y axis). The structure is analyzed without sources. A complete set of modes is obtained in the analysis. There are two families of modes, each producing either vertical or horizontal polarization.

Signal generators are added at a later stage of the analysis. The input ports can be in phase, or in phase opposition. The choice is 180°, forcing odd circular modes. The feeding can be capacitive or inductive, depending on whether monopoles or coils are connected [12].

For vertical polarization, the modes obtained in the electromagnetic analysis correspond to currents that have a magnetic symmetry plane in the YZ plane. To feed these modes it is necessary to use a differential feeding. The currents resemble the function $\cos(n\phi)$ n being an odd number. The maximum of the currents is at the x = 0 coordinate in XY plane.

The characteristics current distribution at resonance frequency of the odd modes and the radiation patterns (E_n) at resonance have been sketched in Fig. 2. Mode J_1 is the fundamental mode, with two current zeros, indicated by dots, this mode generate a broadside pattern. Mode J_3 also is relevant, with the maximum radiation in the z-direction and 6 zeros of current, also indicated by dots. It can be seen that the currents are oriented in the -y direction. The rest are higher order modes that exhibit an increasing number of current nulls along the ring perimeter. Modes J_5 and J_7 are higher order modes with multiple beams.

The characteristic angle (α_n) variation with frequency has been shown in Fig. 3(a). According to the TCM, a characteristic mode is at resonance when its associated characteristic angle is equal to $\alpha_n = 180°$ [8]. Hence, the resonance frequency of the exited characteristic modes of Model A can be determined from Fig. 3(a).

In Fig. 3(b), the percentage of contribution of the odd characteristic modes of Model A to the total radiated power when the antenna is fed with differential excitation have been depicted. Clearly, mode J_1 is dominant at the lowest frequencies, and also from 4.7 to 5.5 GHz. Mode J_3 dominates from 2.5 to 4.7 GHz, and from 7.5 to 8.5 GHz. Mode J_5 is the mode with maximum radiation from 5.5 to 7.5 GHz, and mode J_7 yields the most important contribution to the radiated power from 9.5 to 10 GHz.

Fig. 4(b) shows the simulated S_{11} parameter for Model A. Taking into account the information yielded by the modal analysis of Model A, it can

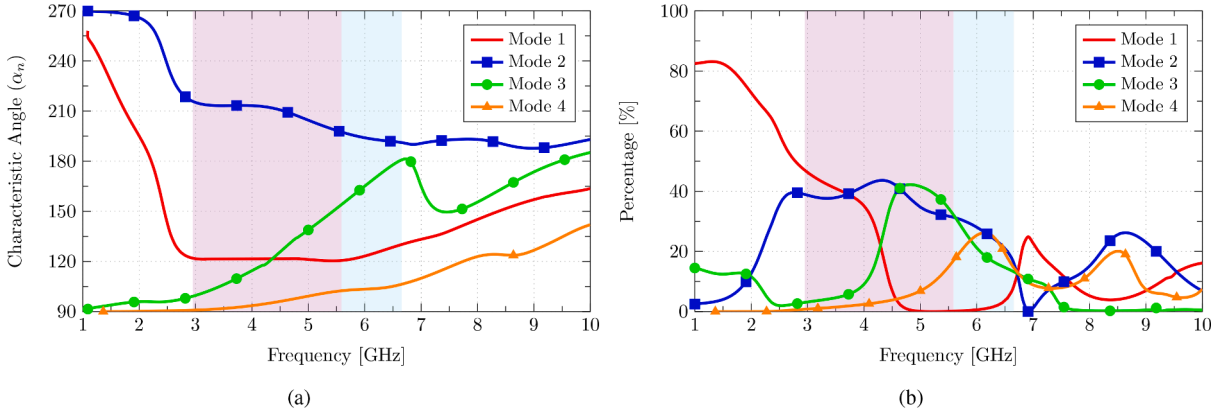

Fig. 5. (a) Characteristic angle variation for the first even modes of Model B, (b) Contribution of the even characteristic modes of Model B to the total radiated power when the antenna is fed with differential excitation.

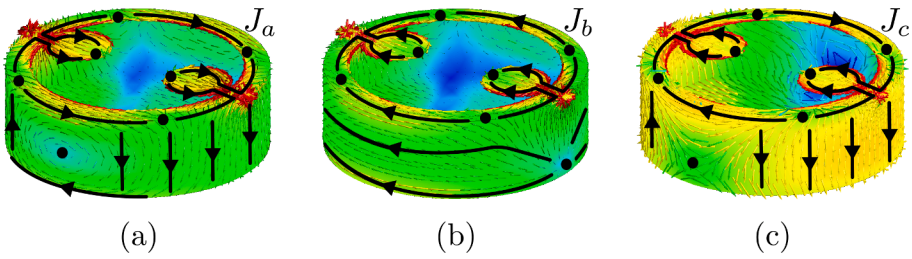

Fig. 6. Current distribution of the modes of Model B at 3.2 GHz. (a) J_1, (b) J_2 and (c) J_3. All three modes have the same current distribution on the top cover as J_3 in model A.

be derived that for the case of the circular ring without the cavity, the first minimum of the S_{11} parameter at 1.5 GHz is caused by the excitation of mode J_1, the second minimum at 4.1 GHz is associated to mode J_3, and the third minimum at 8 GHz results from the combined excitation of J_3, J_1, and other higher order modes.

3. Modal Analysis of a Cavity Backed Antenna

The final design is model B.shown in Fig. 1(b) and (c). This model B adds a circular cavity to Model A to force broadside unidirectional radiation. The height of the cavity is 0.15λ at 3 GHz, and in both models, the perimeter of the circular ring is equal to 2λ at 3 GHz. The modes in the open cylindrical cavity can be analyzed using TCM. An analysis has been performed including both the cavity and the feed structure. In this case a different numbering of the modes would be needed, since there is variation in the z-axis and in the ϕ angle. Sequential numbering of the modes is established as a criterion.

TCM is now going to be used to explain the effect of placing a cavity below the circular ring antenna with differential feeding. Fig. 5(a) shows the characteristic angle variation with frequency for the first characteristic modes of Model B. An analysis has been performed including both the cavity and the feed structure. The modes resonate when the characteristic angle $\alpha = 180^\circ$. Values above 180° are considered capacitive and values below 180° are inductive.

Resonance of a mode is produced when the characteristic angle is 180°, in this case good impedance matching is achieved. Current modes are summed, equivalent to parallel impedances. Good matching can be achieved by a combination of characteristic modes with phases greater than 180° (capacitive) and with phases less than 180° (inductive). The first mode J_1 resonates at 2.2 GHz. There is no resonance between from 3 to 6 GHz, but Model B exhibits wide impedance bandwidth according to Fig. 4(b). It can be understood that the reason is that the characteristic angle curves of modes 1 and 3 are flat and the capacitive and inductive effects are compensated.

The physical explanation is that the bottom of the cavity interacts with the feeding monopoles, creating a capacitive effect that shifts the characteristic angle curves to higher values, avoiding the resonance of modes J_2 and J_3, and reinforcing the radiation of mode J_1 (characteristic angle (α_a) very close to 180°) from 6 to 7 GHz.

Fig. 4(b) shows simulated and measured S_{11} for Model B. This figure also includes t the simulated S_{11} parameter for Model A. The big difference between the two simulations is due to the effect of the ground plane. Impedance bandwidth ($S_{11} < 10$ dB) from 2.8 GHz to 9 GHz is achieved, but this bandwidth will be limited by the stability of the radiation pattern.

Fig. 5(b) presents the percentage of contribution of the characteristic modes to the total radiated power when Model B is fed with differential excitation. Mode J_1 is the main contributor to the total power at the lowest frequencies, however the impedance of J_1 is not well matched to 50 Ohms, so the excitation of this mode does not reflect on the S_{11} parameter of Model B (see Fig. 4(b)). Moreover, from 3 to 6 GHz there is no dominant mode. In this frequency range, the total power is obtained from the combined excitation of several inductive and capacitive characteristic modes. Note that the capacitive mode J_2 does not resonate between 3 and 6 GHz, but it contributes to more than 30% of the total power in this frequency range. Table 2 collects the percentage of power contribution of the modes at two sample frequencies (3.2 GHz and 5.2 GHz) in which the measured S_{11} parameter of Model B is minimum. At 3.2 GHz, the most important contributors are the inductive mode J_1 (44.2 %) and the capacitive mode J_2 (37.6 %). At 5.2 GHz, the modes that contribute more to the total power are the capacitive mode J_2 (33 %) and the inductive mode J_4 (39.8 %).

Table 1
Power contribution of the even modes of Model B.

Model B Mode	3.2 [GHz]	5.2 [GHz]
J_1	44.2%	0%
J_2	37.6%	33%
J_3	12.9%	15.7%
J_4	3.6%	39.8%
J_5	1.05%	9.2%
Others	0.65%	2.3%

Fig. 6 depicts the current distributions of the modes J_1, J_2 and J_3 of Model B at a reference frequency of 3.2 GHz. As observed, in all cases, the current distribution in the upper circular ring corresponds with the current distribution of mode J_3 of Model A. The interaction of the mode J_3 of the ring with the cavity generates a new collection of modes in Model B. The first three cavity modes have the same shape of the current distribution on the top face, they are distinguished by the currents in the side cover of the cylindrical cavity and by the induced currents in the ground plane.

Therefore, the conclusion of this modal analysis is that when a low-profile cavity is included below of a circular ring, it is possible to obtain wide bandwidth by properly combining capacitive and inductive modes. The capacitive and inductive modes compensate each other yielding a very low input reactance from 3 to 6 GHz, that benefits the impedance matching. Furthermore, a stable unidirectional radiation pattern is obtained from this modal combination.

Taking into account the symmetry of the cavity backed circular ring and the orthogonality properties of characteristic modes, it is possible to design dual polarized antenna based on the already explained structure using two orthogonal pairs of differential fed ports as described in next section. (See Table 1).

4. Fabrication and Measurement of the Dual-Polarized Antenna

The low-profile UWB antenna with 4 ports has been fabricated with two types of materials. Copper for the ring, and the four circular patches, and brass for the cylindrical cavity. Fig. 7(a) shows the fabricated prototype and compares the measured and simulated S_{11} parameter. The characterization of the proposed antenna has been carried out using 180° hybrid couplers (not shown in the picture). As can be observed, measured and simulated results are quite similar. The matching band ($S_{11} < -10$ dB) extends from 2.8 GHz to 6 GHz, which corresponds to

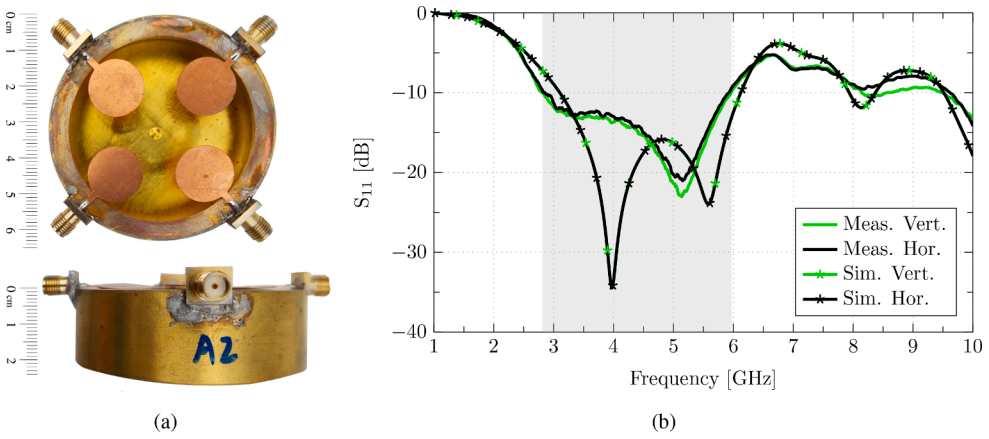

Fig. 7. S_{11} of the low-profile UWB antenna with dual polarization.

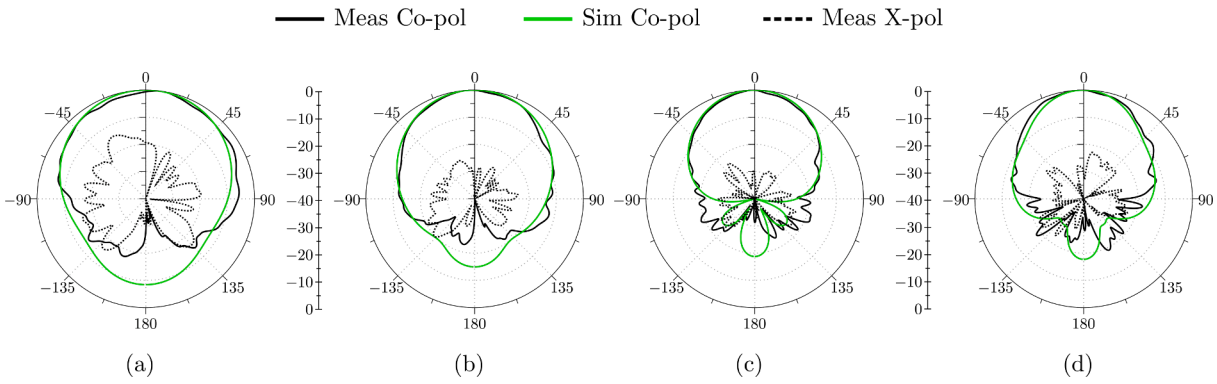

Fig. 8. XZ-plane normalized E-field radiation pattern of the antenna with horizontal polarization: (a) 3 GHz, (b) 4 GHz, (c) 5 GHz and (d) 6 GHz. Simulated (Sim) and measured (Meas) copolar (Co-pol) and crosspolar (X-pol) components.

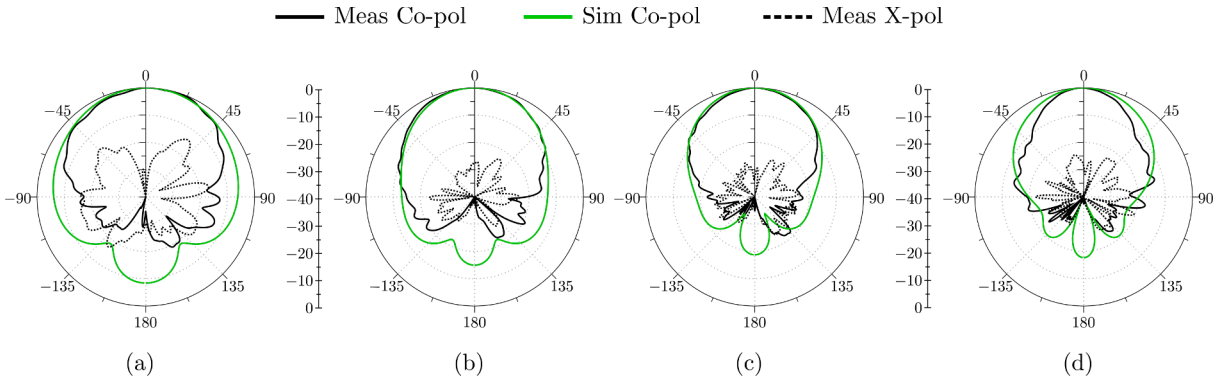

Fig. 9. XZ-plane normalized E-field radiation pattern of the antenna with vertical polarization: (a) 3 GHz, (b) 4 GHz, (c) 5 GHz and (d) 6 GHz. Simulated (Sim) and measured (Meas) copolar (Co-pol) and crosspolar (X-pol) components.

Table 2
Gain of the proposed antenna.

Frequency (GHz)	HORIZONTAL MEAS. Gain XZ (dBi)	SIM. Gain XZ (dBi)	VERTICAL MEAS. Gain XZ (dBi)	SIM. Gain XZ (dBi)
3 GHz	5.50	6.2	4.19	6.20
4 GHz	7.59	8.74	7.24	8.74
5 GHz	8.13	10.11	8.36	10.11
6 GHz	7.89	10.41	8.33	10.41

Table 3
Comparation with published wideband and UWB antennas.

Ref.	Antenna Size (λ_0^3)	S_{11} BW(%)	Polarization
[2]	0.57 × 0.75 × 0.22	43.8	Dual
[3]	0.85 × 0.85 × 0.19	45.45	Dual
[4]	0.86 × 0.86 × 0.16	79.25	Dual
[5]	0.36 × 0.36 × 0.18	45.68	Circular
[6]	0.51 × 0.51 × 0.17	68.9	Circular
[7]	0.70 × 0.70 × 0.18	73.38	Circular
This work	0.64 × 0.64 × 0.15	72.72	Dual

λ_0 represents the free-space wavelength at the lowest frequency.

72% bandwidth. Figs. 8 and 9 show the normalized radiation patterns on the XZ-plane at four frequencies between 3 GHz to 6 GHz, demonstrating that the proposed antenna has a unidirectional radiation pattern for both polarizations. As observed the measured cross-polar radiation pattern is very low in all cases (below −15 dB). The simulated cross-polar component is negligible, so it has not been included. Table 2 demonstrates the good agreement between simulated and measured results for the antenna gain from 3 to 6 GHz for both polarizations.

Finally, a comparison between recently reported antennas with unidirectional radiation pattern and the proposed antenna is given in Table 3. The antennas proposed in references [5–7] are compact and have good bandwidths, but the drawback is that they have only one access port and the possibility of diversity in polarization is lost. The references [2–4] are dual in polarization. The bandwidth achieved in the proposed solution is better than the references [2,3]. The dimensions of the reference [4] are larger and the radiating elements are three-dimensional structures that are difficult to fabricate. Taking into account the comparison shown in Table 3, it can be concluded that the proposed antenna constitutes the best trade-off between antenna size, impedance bandwidth and design simplicity.

5. Conclusion

The TCM has been used to analyze and explain the behavior of a circular ring antenna with differential feeding, and the effect of including a low-profile cavity below this antenna. When differential feeding is used, a stable unidirectional radiation pattern and a broad bandwidth of 72% is obtained with the cavity backed antenna by combining different capacitive and inductive modes that compensate the input reactance. The design has been oriented to 5G operating frequencies at frequencies between 2.8 GHz and 6 GHz. Measurements and simulations demonstrate the feasibility of the prototype, as well as its scalability to other frequency ranges, for example between 1.8 GHz and 3.8 GHz, to cover mobile and WiFi frequencies. Considering the symmetries of the circular ring and the orthogonality of the characteristic modes, a dual-polarization antenna using two pairs of differential fed ports is proposed for indoor 5G base stations. This antenna exhibits a good trade-off between size and impedance bandwidth, and improves the performance of similar antennas already published.

Declaration of Competing Interest

The authors declare that they have no known competing financial interests or personal relationships that could have appeared to influence the work reported in this paper.

Acknowledgement

This work has been supported by the Spanish Ministry of Science, Innovation, and Universities (Ministerio de Ciencia, Innovación y Universidades) under the program PID2019-107885 GB-C3-2

References

[1] Kumar S, Dixit AS, Malekar RR, Raut HD, Shevada LK. Fifth generation antennas: a comprehensive review of design and performance enhancement techniques. IEEE Access 2020;8:163568–93.
[2] Lee H, Lee B. Compact broadband dual-polarized antenna for indoor MIMO wireless communication systems. IEEE Trans. Antennas Propag. 2016;64(2):766–70.
[3] Wen L-H, Gao S, Mao C-X, Luo Q, Hu W, Yin Y, Yang X. A wideband dual-polarized antenna using shorted dipoles. IEEE Access 2018;6:39725–33.
[4] Feng B, Tu Y, Chung KL, Zeng Q. A beamwidth reconfigurable antenna array with triple dual-polarized magneto-electric dipole elements. IEEE Access 2018;6:36083–91.
[5] He Y, He W, Wong H. A wideband circularly polarized cross-dipole antenna. IEEE Antennas Wireless Propag. Lett. 2014;13:67–70.
[6] Tran HH, Park I, Nguyen TK. Circularly polarized bandwidth-enhanced crossed dipole antenna with a simple single parasitic element. IEEE Antennas Wireless Propag. Lett. 2017;16:1776–9.
[7] Li M, Luk K-M. A wideband circularly polarized antenna for microwave and millimeter-wave applications. IEEE Trans. Antennas Propag. 2014;62(4):1872–9.
[8] Cabedo-Fabres M, Antonino-Daviu E, Valero-Nogueira A, Bataller MF. The theory of characteristic modes revisited: A contribution to the design of antennas for modern applications. IEEE Antennas Propag. Mag. 2007;49(5):52–68.
[9] C.R. Peñafiel-Ojeda, M. Cabedo-Fabrés, E. Antonino-Daviu, M. Ferrando-Bataller, Design of an unidirectional UWB cavity backed antenna, in: Numerical Electromagnetic and Multiphysics Modeling and Optimization for RF, Microwave, and Terahertz Applications (NEMO), 2017 IEEE MTT-S International Conference on, IEEE, 2017, pp. 28–30.
[10] Harrington R, Mautz J. Theory of characteristic modes for conducting bodies. IEEE Trans. Antennas Propag. 1971;19(5):622–8.
[11] E. Antonino-Daviu, M. Cabedo-Fabres, M. Gallo, M. Ferrando-Bataller, M. Bozzetti, Design of a multimode mimo antenna using characteristic modes, in: 2009 3rd European Conference on Antennas and Propagation, 2009, pp. 1840–1844.
[12] Antonino-Daviu E, Cabedo-Fabrés M, Sonkki M, Mohamed-Hicho NM, Ferrando-Bataller M. Design guidelines for the excitation of characteristic modes in slotted planar structures. IEEE Trans. Antennas Propag. 2016;64(12):5020–9.